Theoretical Investigation of Collisions of Aligned Atoms: Ca($4s4f\ ^1F$)+He

A. P. Hickman,[1] J. J. Portman,[1] S. Krebs,[2,*] and W. Meyer[2]
[1]*Molecular Physics Laboratory, SRI International, Menlo Park, California 94025*
[2]*Facultät für Chemie, Universität Kaiserslautern, 67663 Kaiserslautern, Germany*
(Received 30 August 1993)

Cross sections for inelastic collisions of aligned, excited atoms are calculated using *ab initio* molecular potential curves and couplings and a fully quantum mechanical scattering treatment. Agreement with currently available data is reasonable. The cross sections for specific transitions exhibit strong, energy-dependent oscillations, which are attributed to an interference effect.

PACS numbers: 34.50.Pi

Recent developments in experimental techniques have led to the investigation of collision processes involving atoms prepared initially in aligned states [1]. In a series of elegant experiments [2–5], Leone's group has investigated such collisions using excited Ca atoms and has found a strong dependence of specific inelastic cross sections on the initial alignment. Analysis of these results has been limited by the lack of reliable potential curves; available calculations [6] have been based on model potentials. In this Letter, we report a full analysis of an aligned atom collision based on *ab initio* potentials.

We consider the process

$$\mathrm{Ca}(4s4f\ ^1F)+\mathrm{He}\rightarrow \mathrm{Ca}(4p^2\ ^1S)+\mathrm{He}. \quad (1)$$

For this system, Driessen, Smith, and Leone [5] have performed the following experiment. The initial Ca atom is prepared in a well defined state, whose quantization axis is related to the directions of the polarizations of the lasers used to prepare the state. Specifically, ^1F states ($J=3$) whose angular wave function is $|J0\rangle$ or $(|J1\rangle - |J-1\rangle)/\sqrt{2}$ can be prepared. The excited atoms interact with a beam of He atoms incident at an angle β with respect to the quantization axis, and collisions cause transitions to several final Ca states. Transitions to the $4p^2\ ^1S$ are detected by monitoring fluorescence from that state. The experimental signal is the ^1S fluorescence as a function of β; this signal is proportional to a cross section $\sigma(\beta)$ for process (1).

For the conventional analysis of scattering experiments, one usually defines the z axis to coincide with the initial velocity vector of the relative motion. From this point of view, the information contained in $\sigma(\beta)$ could also be expressed as a set of cross sections σ_M, $M=0,1,\ldots,J$, where M is the projection of the initial atomic angular momentum J on the z axis. (Note $\sigma_M=\sigma_{-M}$.) The experimental signal $\sigma(\beta)$ is related to the σ_M by

$$\sigma(\beta)=\sum_M \lambda_M(\beta)^2\sigma_M. \quad (2)$$

The coefficients $\lambda_M(\beta)$ are determined from rotation matrix elements and from the initial state angular wave function [4]. Driessen, Smith, and Leone have given $\lambda_M(\beta)$ explicitly for two different arrangements of their laser polarizations. They have measured two sets of σ_M corresponding to two slightly different energy distributions.

The first step of the theoretical analysis was to perform the necessary electronic structure calculations. Figure 1 shows some of the adiabatic potentials, which were calculated at the configuration interaction (CI) level using the core polarization potential of Mueller, Flesch, and Meyer [7], and a basis set with 15s, 9p, 8d, and 5f Gaussian-type orbitals. The calculated Ca excitation energies generally agree with experiment within about 150 cm^{-1}, and the spacings between the states near the ^1F state are correct to within 20 cm^{-1}. Radial coupling matrix elements were calculated by numerical differentiation. The most important of these couplings are also shown in Fig. 1. Angular coupling terms (the matrix elements of L_x and L_y) were also calculated. Details of the electronic structure calculations will be published separately [8].

The behavior of the potentials at long range is due mainly to exchange terms between the Rydberg electron and He and reflects the radial probability density of the

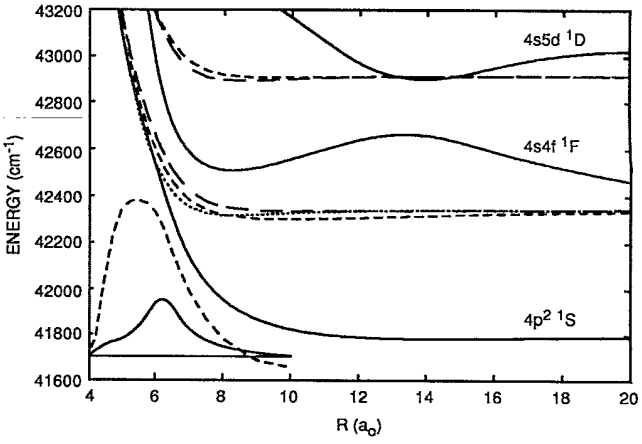

FIG. 1. Selected *ab initio*, adiabatic potential curves for CaHe, for Σ (——), Π (---), Δ (--), and Φ (····) symmetry. The inset at lower left shows $\langle F\Pi|L_x|S\Sigma\rangle$ (---), which governs the rotational coupling, and the radial coupling term $\langle F\Sigma|d/dR|S\Sigma\rangle$ (——).

0031-9007/94/72(12)/1814(4)$06.00

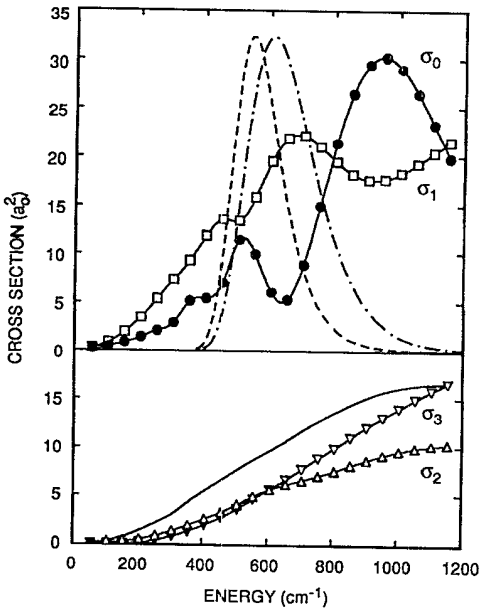

FIG. 2. Calculated cross sections σ_M. In the upper panel, the collision energy distributions are shown for the initial states $|J0\rangle$ (-·-) and $(|J1\rangle-|J-1\rangle)/\sqrt{2}$ (---). In the lower panel, the solid line is the average cross section.

outer electron. For Σ states, the maxima of the ^1F and ^1D curves near $14a_0$ and $20a_0$ correlate with the corresponding $4f$ and $5d$ wave functions; what appears to be an avoided crossing at $14a_0$ arises instead from a node in the $5d$ wave function. For non-Σ states, the He lies on a nodal plane and the electronic interaction is much smaller.

Inspection of the adiabatic curves in Fig. 1 indicates two possible transition mechanisms connecting the F and S levels: radial coupling in the range $(5-8)a_0$ between the two Σ potentials, and rotational coupling in the same region between the $F\Pi$ and the $S\Sigma$ potentials. The latter coupling arises because for $R \lesssim 8a_0$, the adiabatic Σ state correlating to the ^1S asymptote has significant ^1F character.

The next step was to solve the coupled channel scattering equations. In a diabatic representation (i.e., using an atomiclike basis), these equations are written

$$\left[\frac{-\hbar^2}{2\mu}\frac{d^2}{dR^2}+V(R)-E\right]F=0, \tag{3}$$

where μ is the reduced mass, $V(R)$ is a coupling matrix including electronic interactions and the centrifugal terms, and E is a diagonal matrix of the channel energies. $V(R)$ is determined from the *ab initio* results using the matrix $C(R)$ that transforms the adiabatic wave functions $|i\rangle$ to the desired diabatic representation. $C(R)$ was found by diagonalizing $\langle i|J^2|j\rangle$ to recover states of well defined J^2 corresponding to atomic states. (Note $J^2=L^2$ for our singlet states.) The diagonal elements of $V(R)$ were shifted slightly to match the atomic energies; the off-diagonal elements were not changed. The rotational coupling terms obtained in the *ab initio* calculations were transformed using $C(R)$ and included in $V(R)$.

TABLE I. Partial cross sections σ_M, normalized so that $\bar{\sigma}=[\sigma_0+2(\sigma_1+\sigma_2+\sigma_3)]/7=1$. The theoretical values of $\bar{\sigma}$ were 10.69 a.u. [$|J0\rangle$] and 9.17 a.u. [$(|J1\rangle-|J-1\rangle)/\sqrt{2}$].

	$\|J0\rangle$		$(\|J1\rangle-\|J-1\rangle)/\sqrt{2}$	
M	Theory	Experiment	Theory	Experiment
0	1.04	1.34(1)	1.01	1.46(2)
1	1.78	1.24(2)	1.87	1.39(1)
2	0.56	0.75(2)	0.56	0.83(3)
3	0.64	0.84(2)	0.57	0.55(10)

The cross sections are defined in terms of the T matrix elements, which are determined by solving Eq. (3). The result is

$$\sigma_M=\frac{\pi}{k^2}\sum_P(2P+1)\sum_{N'}\left|\sum_N i^N\langle JMP-M|N0\rangle T^P_{\alpha'J'N',\alpha JN}\right|^2, \tag{4}$$

where N is the orbital angular momentum of the Ca-He relative motion, $P=J+N$, $\langle\cdots\rangle$ is a Clebsch-Gordan coefficient, and αJ and $\alpha' J'$ denote the initial ^1F and final ^1S states.

Figure 2 shows the calculated cross sections σ_M for collision energies 60 to 1100 cm^{-1}. The results reported are based on including the F and S levels; additional channels did not change the results significantly. The most striking feature of these results is the strong energy dependence of σ_0 and σ_1, which contrasts with the smooth behavior of the cross section averaged over M. The origin of the oscillations will be discussed below. We convoluted the cross sections with the experimental energy distributions [5]. [We used a peak at 613 cm^{-1} and FWHM of 210 cm^{-1} for the $|J,0\rangle$ state and a peak at 540 cm^{-1} and FWHM of 160 cm^{-1} for the $(|J1\rangle-|J-1\rangle)/\sqrt{2}$ state.] The convoluted cross sections are compared with the corresponding experimental values in Table I and in Fig. 3. The energy-averaged cross sections shown in Fig. 3 agree with experiment with respect to the relative size of σ_0 and σ_1 compared to σ_2 and σ_3, but there is a discrepancy in the ordering of σ_0 and σ_1. This ordering depends on the phase of the oscillations of σ_0 and σ_1 (see Fig. 2). The oscillations are an interference effect sensitive to the calculated potentials; this sensitivity may account for the discrepancy.

To understand the origin of the oscillations, we examine the collision dynamics in more detail. To analyze the contributions of the radial and rotational coupling mechanisms mentioned above, one needs to know the amplitude for the atoms to "choose" the Σ or the Π state in a particular collision. We calculate this amplitude by formulating a time-dependent semiclassical theory for the

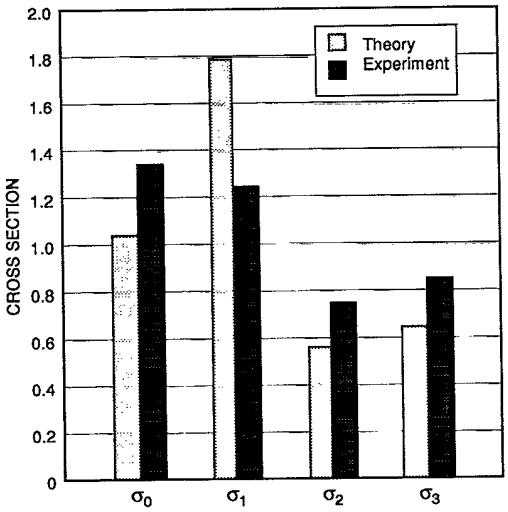

FIG. 3. Comparison of energy-averaged cross sections with experiment (Ref. [5]) for initial state $|J0\rangle$.

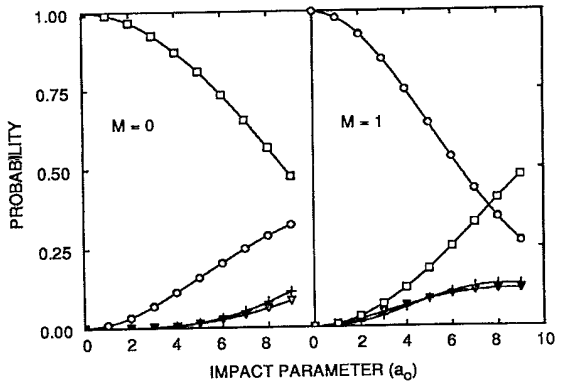

FIG. 4. The probabilities $|f_{M\Lambda}|^2$ connecting SF states $M=0$ and 1 with σ (□), Π (○), Δ (∇), and Φ (+) BF states.

evolution of the initial states of fixed M (in the space-fixed frame) into specific molecular states labeled by Λ (Σ, Π, etc.). The essential points of the theory can be illustrated by describing the two state limit, in which an initial level ($J=1$) is correlated with a Σ and a Π potential curve. Our approach differs from Grosser's [9]. We evaluate the coupling matrix V using a space-fixed (SF) coupled angular momentum representation [10]. The total angular momentum P is conserved, and the channels are labeled by N, which has two possible values, $N=P\pm 1$. Then V can be written

$$\bar{V}(R)-\hbar bv/R^2,\quad [V_\Sigma(R)-V_\Pi(R)]/2,$$
$$[V_\Sigma(R)-V_\Pi(R)]/2,\quad \bar{V}(R)+\hbar bv/R^2. \tag{5}$$

$\bar{V}(R)=[V_\Sigma(R)+V_\Pi(R)]/2+P(P+1)/2\mu R^2$ is the average electronic plus the average centrifugal energy. The splitting between the diagonal energies follows from the relation $N_\pm(N_\pm+1)\sim P(P+1)\pm 2P$. We have taken the limit $P\gg 1$ and expressed the coupling in terms of the velocity v and impact parameter b ($b=\hbar P/\mu v$). We introduce time dependence by invoking a straight line trajectory $R=[b^2+(vt)^2]^{1/2}$ for the nuclear motion. This model should be reliable, since the transitions of interest take place at long range, where the potential is weak, but more elaborate methods [11] are available.

We calculate the amplitude for the atoms to be in each of the possible adiabatic states as a function of time during the collision. At $t=-\infty$ (large R) the adiabatic states are the coupled SF states. At smaller values of R, the off-diagonal elements in Eq. (5) become large compared to the splitting of the diagonal elements, and the molecular or body-fixed (BF) states labeled by Λ are the adiabatic states. The transition between these two regimes occurs near R_x, the value of R where the off-diagonal term in Eq. (5) is equal to one-half of the difference of the diagonal terms. (Note that R_x depends on b.) We calculated the transition probabilities by integrating from $t=-\infty$ to the time at which the atoms first reach a distance of $12a_0$. There the BF Σ and Π states are well defined, but transitions to the ^1S state have not yet taken place.

A crucial step is the preparation of the initial wave function ($t=-\infty$) in terms of the SF basis functions whose quantum numbers are J, N, P, and M_P. We must construct a state with well defined J, M_J (denoted M), P, and M_P. Since $M_N=0$ initially in a collision, $M_P=M$. Using Clebsch-Gordon coefficients we express the desired initial state as

$$|J,M,P,M\rangle=\sum_N\langle JMP-M|N0\rangle|JNPM\rangle. \tag{6}$$

The calculations for the ^1F ($J=3$) initial level included four states $|J0\rangle$ and $[|JM\rangle+(-1)^M|J-M\rangle]/\sqrt{2}$ for $M=1,2,3$. We solved the semiclassical equations by subdividing the time domain into several intervals and using Light's [12] Magnus propagator in each interval. We show in Fig. 4 the squares of the amplitudes $f_{M\Lambda}$ that an initially prepared $M=0$ or $M=1$ state becomes, after passing through the coupling region, a Σ, Π, Δ, or Φ state. The collision energy was 540 cm^{-1}. The behavior of the numerical results as $b\to 0$ is what one would expect physically as the angular velocity of the internuclear axis vanishes and the BF and SF frames coincide.

These results for $f_{M\Lambda}$ provide a framework for interpreting the oscillations in σ_0 and σ_1. We write $\sigma_M=2\pi\int P_M(b)b\,db$, where two processes contribute to the transition probabilities P_M:

$$\lambda P_M(b)=|f_{M\Sigma}A_\Sigma+f_{M\Pi}A_\Pi|^2. \tag{7}$$

The factor λ, which is 1 if $M=0$ and 2 if $M\geq 1$, arises from the linear combination of $|JM\rangle$ and $|J-M\rangle$ states. A_Σ (A_Π) depends on b and is the amplitude for a transition from the Σ (Π) state to the ^1S state. The right-hand

side of Eq. (7) can be written as

$$|f_{M\Sigma}A_\Sigma|^2+|f_{M\Pi}A_\Pi|^2+2\mathrm{Re}f^*_{M\Sigma}f_{M\Pi}A^*_\Sigma A_\Pi. \quad (8)$$

The last term can lead to interference effects in the σ_M. However, the sum of these terms over M vanishes because $f_{M\Lambda}$ is unitary. Equation (7) can therefore account for oscillations in each σ_M as well as the smooth behavior of the average.

The results shown in Fig. 4 confirm that at large impact parameters, a ^1F $M=0$ state can evolve either into a Σ or a Π state, both of which are coupled to the ^1S final state. Indeed, our coupled channel calculations of the partial cross sections for $M=0$ to ^1S transitions exhibit a complicated oscillatory dependence on energy and impact parameter. As further evidence for the interference effect, we note that suppressing the rotational coupling between the ^1F Π curve and the ^1S curve eliminates the oscillations in the energy dependence.

The interference effect is related to the long range barrier in the ^1F Σ potential shown in Fig. 1. There is a significant phase difference between trajectories that follow the Σ curve and surmount the barrier, and those that follow the flat Π curve. A model calculation attributing the phase difference between A_Σ and A_Π in Eq. (8) to this effect matches the oscillatory behavior of σ_0 very well. There is another effect of the barrier. At collision energies E less than the barrier height (~ 320 cm^{-1}), trajectories that follow the Σ state will generally not penetrate to the region at small R where transitions to the ^1S state can take place. We expect σ_0 to be strongly suppressed then, because the $M=0$ initial states evolve preferentially into Σ states. Figure 2 confirms that for $E<300$ cm^{-1}, σ_1 is the largest partial cross section, and can be 2–2.5 times larger than the other σ_M. We also notice in Fig. 2 that the oscillations in σ_0 begin at 300–350 cm^{-1}, the energy range at which trajectories that begin in the $M=0$ state can first surmount the barrier. The quantum mechanical results revealed evidence of orbiting resonances in this energy range.

Our semiclassical results can be compared with the well known locking radius model (LRM) [2]. This model assumes that when the internuclear distance approaches some value R_L, the initial SF wave function is projected onto BF states, which subsequently remain "locked" to the rotating molecular axis. The angle γ between the SF and BF frames at R_L is given by $\sin\gamma=b/R_L$. The predictions of the LRM for the $f_{M\Lambda}$ for states of arbitrary J can be expressed in terms of rotation matrices depending on the Euler angles $(0,\gamma,0)$. The results for $M=0$ are $f_{0\Sigma}=P_J(\cos\gamma)$ and $f_{0\Pi}=\sqrt{8\pi/(2J+1)}Y_{J1}(\gamma,0)$. We tried to fit our calculated $f_{M\Lambda}$ using these formulas, treating R_L as an adjustable parameter. For $R_L=27.4a_0$, the fit by $|f_{0\Sigma}|^2$ was excellent over the entire range of impact parameters ($b<9a_0$) that contribute to the ^1F to ^1S transition. However, the fit by $|f_{0\Pi}|^2$, using the same value of R_L, was accurate only for $b<(3$–$4)a_0$. Moreover, the LRM did not properly model the locking process. The value of R_L that fit $|f_{0\Sigma}|^2$ was not close to the value of R at which the transition from an $M=0$ SF state to a well defined BF Σ wave function took place. The semiclassical results clearly showed that those transitions occurred in a broad range around R_x (defined above), which was $(40$–$52)a_0$, for $1a_0\le b\le 9a_0$.

In conclusion, we have analyzed collisions of aligned Ca($4s4f$ ^1F) atoms with He. The key results are prominent oscillations in the energy dependence of σ_0 and σ_1, which have been quantitatively modeled as an interference phenomenon, and strong enhancement of σ_1 at low collision energies. Further experimental studies are needed to confirm these predictions.

A.P.H. was supported by NSF Grant No. PHY-9204879 and completed part of this work at Kaiserslautern University supported by SFB 92. J.J.P. was supported by NSF Grant No. PHY-9300247 (an REU site grant at SRI). S.K. and W.M. were supported by the DFG. A.P.H. acknowledges helpful discussions or correspondence with M. Dalberth, S. Leone, C. Smith, and G. Schatz.

*Present address: Universität Wuppertal, Fachbereich 9, Theoretische Chemie, D-42097, Wuppertal, Germany.

[1] I. V. Hertel, H. Schmidt, A. Baehring, and E. Meyer, Rep. Prog. Phys. **48**, 375 (1985).
[2] M. O. Hale, I. V. Hertel, and S. R. Leone, Phys. Rev. Lett. **53**, 2296 (1984).
[3] W. Bussert, D. Neuschaefer, and S. R. Leone, J. Chem. Phys. **87**, 3833 (1987).
[4] R. L. Robinson, L. J. Kovalenko, C. J. Smith, and S. R. Leone, J. Chem. Phys. **92**, 5260 (1990).
[5] J. P. J. Driessen, C. J. Smith, and S. R. Leone, Phys. Rev. A **44**, 1431 (1991); J. Phys. Chem. **95**, 8163 (1991).
[6] B. Pouilly and M. H. Alexander, Chem. Phys. **145**, 191 (1990).
[7] W. Mueller, J. Flesch, and W. Meyer, J. Chem. Phys. **80**, 3297 (1984).
[8] S. Krebs and W. Meyer (to be published).
[9] J. Grosser, J. Phys. B **14**, 1449 (1981).
[10] G. C. Shatz, L. J. Kovalenko, and S. R. Leone, J. Chem. Phys. **91**, 6961 (1989).
[11] M. H. Alexander, J. Chem. Phys. **96**, 6672 (1992).
[12] J. C. Light, J. Chem. Phys. **66**, 5241 (1977).